GBMF5076. M.M.K. acknowledges generous support from the David and Lucille Packard Foundation.

Based on observations obtained with the Samuel Oschin Telescope 48 inch and the 60 inch Telescope at the Palomar Observatory as part of the ZTF project. ZTF is supported by the National Science Foundation under grant no. AST-1440341 and a collaboration including Caltech, IPAC, the Weizmann Institute for Science, the Oskar Klein Centre at Stockholm University, the University of Maryland, the University of Washington, Deutsches Elektronen-Synchrotron and Humboldt University, Los Alamos National Laboratories, the TANGO Consortium of Taiwan, the University of Wisconsin at Milwaukee, and Lawrence Berkeley National Laboratories. Operations are conducted by COO, IPAC, and UW. SEDM is based upon work supported by the National Science Foundation under grant no. 1106171. The ZTF forced-photometry service was funded under Heising-Simons Foundation grant 12540303 (PI: Graham). Some of the data presented herein were obtained at the W.M. Keck Observatory, which is operated as a scientific partnership among Caltech, the University of California, and the National Aeronautics and Space Administration. The Observatory was made possible by the generous financial support of the W.M. Keck Foundation. The authors wish to recognize and acknowledge the very significant cultural role and reverence that the summit of Maunakea has always had within the indigenous Hawaiian community. We are most fortunate to have the opportunity to conduct observations from this mountain. Based on observations made with NOT (operated by the Nordic Optical Telescope Scientific Association at Observatorio del Roque de los Muchachos, La Palma, Spain, of Instituto de Astrofisica de Canarias).

A.G.Y.'s research is supported by the European Union via European Research Council grant no. 725161, the ISF GW Excellence Center, an IMOS space infrastructure grant, and BSF/Transformative and GIF grants, as well as The Benoziyo Endowment Fund for the Advancement of Science, the Deloro Institute for Advanced Research in Space and Optics, The Veronika A. Rabl Physics Discretionary Fund, Paul and Tina Gardner, Yeda-Sela, and the WIS–CIT joint research grant. A. G.Y. is a recipient of the Helen and Martin Kimmel Award for Innovative Investigation. A.Y.Q.H. is supported by a National Science Foundation Graduate Research Fellowship under grant no. DGE-1144469 and by the GROWTH project funded by the National Science Foundation under PIRE grant no. 1545949. R.L. is supported by a Marie Skłodowska-Curie Individual Fellowship within the Horizon 2020 EU Framework Programme for Research and Innovation (H2020-MSCA-IF-2017-794467). Foscgui is a graphic user interface aimed at extracting SN spectroscopy and photometry obtained with FOSC-like instruments. It was developed by E. Cappellaro. A package description can be found at http://sngroup.oapd.inaf.it/foscgui.html.

Facilities: PO:1.2 m (ZTF), PO:1.5 m (SEDM), Hale (DBSP, WaSP), NOT: ALFOSC, THO: ALPY200, Keck: I (LRIS).

Software: `astropy` (Astropy Collaboration et al. 2013), `matplotlib` (Hunter 2007), `scipy` (Virtanen et al. 2020), `pandas` (McKinney 2010), `SExtractor` (Bertin & Arnouts 1996), `scamp` (Bertin 2006), `SWarp` (Bertin et al. 2002), `PSFEx` (Bertin 2011), `pysedm` (Rigault et al. 2019), `pyraf-dbsp` (Bellm & Sesar 2016), `lpipe` (Perley 2019), `simsurvey` (Feindt et al. 2019).

Appendix
Transients in the Control Sample

Here we discuss the photometric and spectroscopic properties of the transients that pass the selection criteria for follow-up but do not exhibit high [Ca II]/[O I] ratios in their nebular-phase spectra. We summarize the photometric and spectroscopic properties of these transients in Table 1. The control sample consists of four SNe Ib, five SNe Ic, one SN Ic-BL, two SNe Ib/c, and three SNe Ia. Figure 28 shows the forced-photometry light curves of these transients, while Figure 29 shows a collage of the spectroscopic data for each object. The complete log of the spectroscopic follow-up for these objects is presented in Table 3, which will be released on WISeREP together with the photometry upon publication. We plot the original reduced spectra for the spectroscopy epochs near peak light for each object. For the nebular-phase spectra, we show the original reduced spectra for events that do not have large host contamination. For other nebular spectra, we attempt to fit a polynomial to the underlying host continuum to subtract the host features and show the subtracted spectrum to highlight the broad nebular emission features of [O I] and [Ca II]. In cases where the host background is not smooth and has features sharper than ≈1000 Å (usually the case for S0/E-type galaxies) such that the nebular emission features are not easily measurable, we attempt more careful host subtraction using `superfit` (Howell et al. 2005). In these cases, the spectrum figures show the unsubtracted spectra, and the `superfit`-subtracted spectra are shown in Figure 30.

In addition to the objects discussed here, we note the case of the peculiar SN 2019ehk in the galaxy M100. SN 2019ehk was reported to the TNS by Grzegorzek (2019) and an early spectrum was reported by Dimitriadis et al. (2019), which exhibited a reddened featureless continuum with "flash"-ionized lines (see, e.g., Gal-Yam et al. 2014) of He II λ4686 and Hα. We obtained follow-up spectra of the event near peak light with DBSP, which show a reddened continuum with strong photospheric He absorption features and weaker H features, similar to Type IIb SNe. Specifically, the peak light spectra show signatures of Hβ and Hγ absorption together with a flat-bottomed feature near Hα blended with the nearby He I λ6678 line. The flat-bottomed Hα feature is characteristic of several well-studied SNe IIb like SN 2001ig (Silverman et al. 2009) and SN 2011dh (Marion et al. 2014). Curiously, this object shows strong [Ca II] lines in our early nebular-phase spectrum from SEDM and LRIS, similar to several Ca-rich transients in this sample. However, the clear presence of H in the early flash spectra and at peak light excludes it from our sample. Additionally, the deep Na I D absorption detected in its spectrum suggests significant host reddening by $A_V \gtrsim 3$ mag, making it intrinsically luminous ($M_p \lesssim -17$). This object may be similar to the Type IIb iPTF 15eqv, which exhibits high [Ca II]/[O I] in late-time spectra (Milisavljevic et al. 2017), and we defer the discussion of this object to future work.

A.1. Spectroscopic Classification

We summarize the detection, environment, and properties of each transient in the control sample, and particularly highlight how we exclude it from the group of Ca-rich gap transients. In

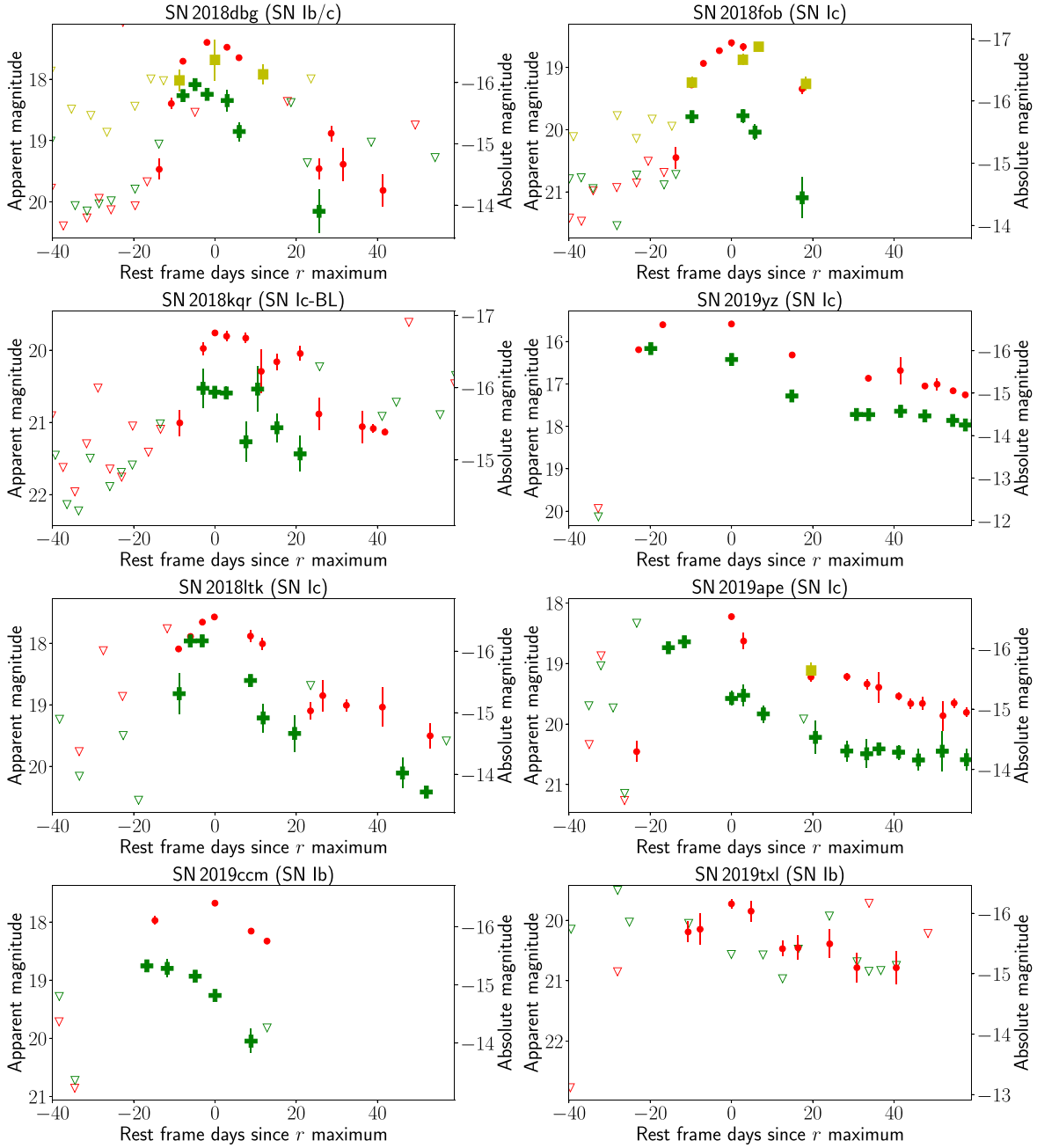

Figure 28. Forced-photometry light curves of each object in the control sample that does not pass the [Ca II]/[O I] threshold defined in the sample. Each panel shows the photometric evolution near peak for the transient indicated in the figure title. We include photometry in *gri* filters from ZTF and phase is defined with respect to time from the *r*-band peak. Red circles denote *r*-band photometry, green plus symbols indicate *g*-band photometry, and yellow squares indicate *i*-band photometry. Hollow inverted triangles denote 5σ upper limits at the location of the transient.

the next section, we use this discussion to compare the properties of these transients to those of the Ca-rich sample.

SN 2019ccm was found on top of the spiral arm of an Sa-type galaxy at $z = 0.015$ and peaked at an absolute magnitude of $M_r \approx -16.4$ mag (without correcting for its host extinction). A spectrum taken at peak light shows characteristic features of an SN Ib at peak on the red side (the blue-side spectrum was not recorded due to a readout issue on the LRIS detector), as well as a deep Na I D feature at the host redshift, suggesting that the low luminosity is partly due to host extinction. An LRIS spectrum taken ≈180 days after peak shows [O I] and [Ca II] emission of nearly equal strengths, ruling out a Ca-rich classification. We note that the [Ca II]/[O I] ratio (≈1.18) is likely overestimated because the significant host extinction would only increase the observed ratio.

SN 2019txl was found on the arm of a spiral galaxy at $z = 0.034$ and peaked at an absolute magnitude of $M_r \approx -16.2$ mag. The peak light spectrum shows typical features of an SN Ib at peak, together with clear Na I D absorption at the host redshift, confirming it as a reddened normal SN Ib. A nebular-phase spectrum taken ≈+330 days from peak shows clear signatures of [O I] and [Ca II] emission with a [Ca II]/[O I] of ≈0.9 (without correcting for host extinction), thus excluding it from the Ca-rich sample.

SN 2019txt was found on the disk of a nearly edge-on disk galaxy at $z = 0.026$ and peaked at an absolute magnitude of

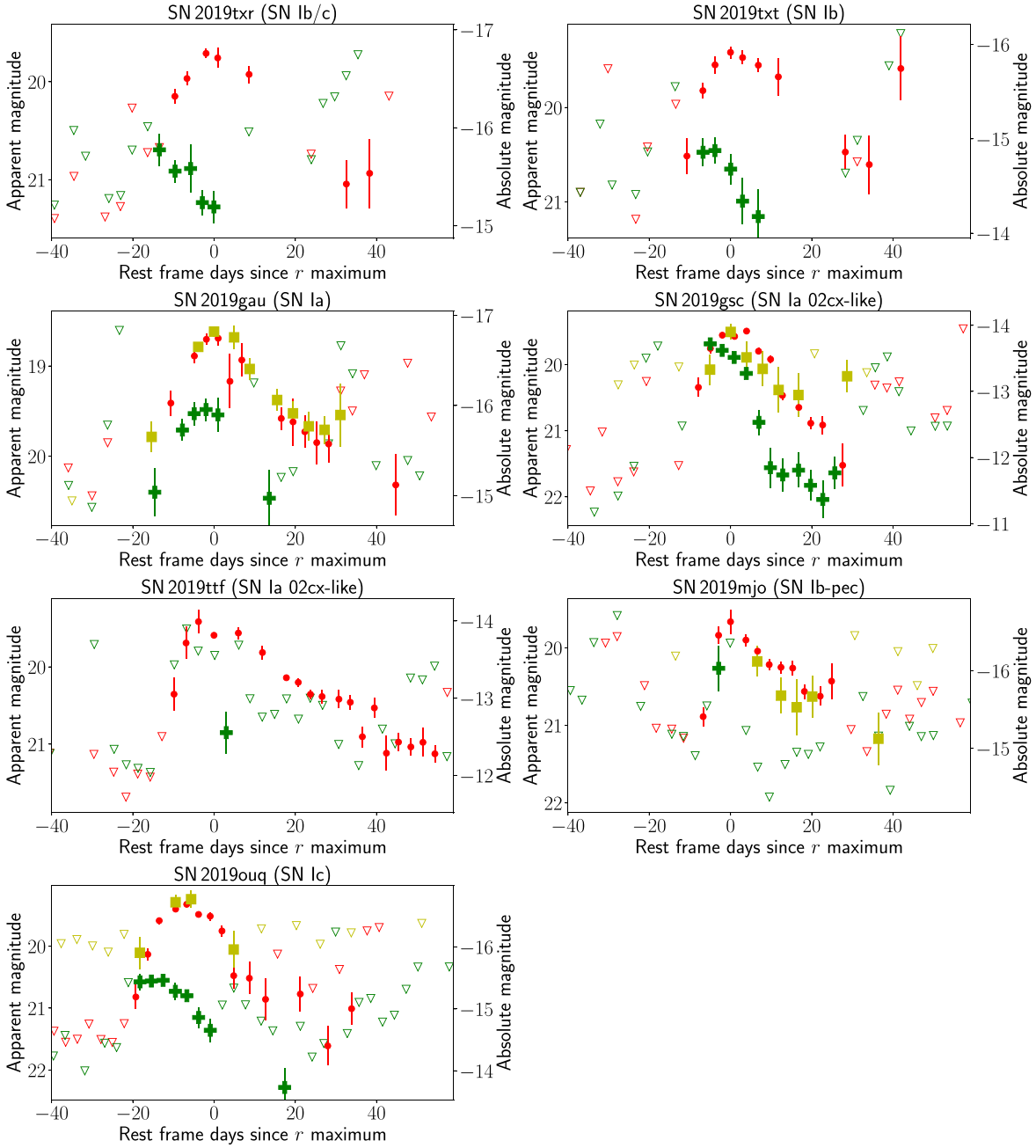

Figure 28. (Continued.)

$M_r \approx -15.9$ mag. The peak light spectrum is relatively noisy but still clearly shows features of an SN Ib at peak, as well as prominent Na I D absorption at the host redshift, consistent with a reddened SN Ib. The nebular-phase spectrum at ≈220 days from peak light shows clear [O I] and [Ca II] emission with [Ca II]/[O I] of ≈1.3 without host extinction correction, thus excluding it from the Ca-rich sample.

SN 2019mjo stands out as a peculiar SN Ib found in the outskirts of an elliptical galaxy at $z \approx 0.041$. Its peak light spectrum is reddened with strong He lines and it exhibits a very slow transition in spectroscopic properties. The source does not turn nebular even in our latest spectrum at ≈+180 days from peak light, and hence does not satisfy our criterion for a fast nebular-phase transition. We defer conclusions about the nature of this event to a forthcoming publication that will present the full data set on this source (K. De et al. 2020, in preparation).

SN 2018dbg was found close to the nucleus of a grand spiral host galaxy at $z \approx 0.015$, peaking at an absolute magnitude of $M_r \approx -16.6$ mag. We were unable to secure a peak light spectrum of SN 2018dbg, but secured a spectrum at ≈35 days after peak, where the spectrum was still dominated by strong photospheric-phase lines of O, Ca II, and possibly He I. Using `superfit` (Howell et al. 2005) to subtract the underlying continuum, we found an excellent match to the spectrum of the Type Ib SN 1990U at ≈+41 days after peak, consistent with the photometric phase (≈+30 days). We thus classify it as an SN Ib/c. Since all Ca-rich gap transients start exhibiting strong nebular [Ca II] emission features at this phase, this object does

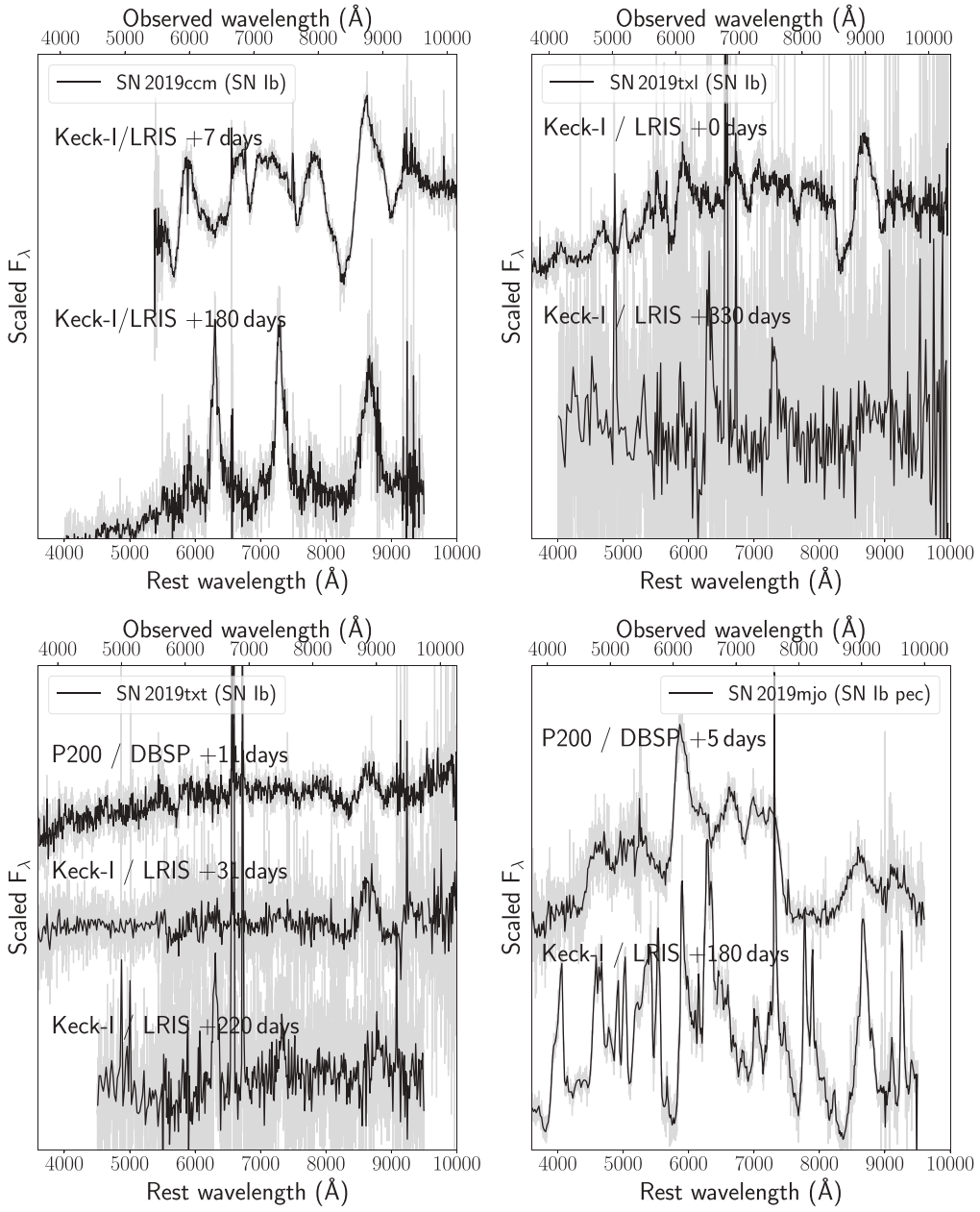

Figure 29. Photospheric- and nebular-phase spectra of objects in the control sample that do not pass either the early nebular-phase transition criterion or the nebular-phase [Ca II]/[O I] threshold defined in the sample (see Appendix). Each panel shows one object with its name and classification indicated in the legend. Gray lines show the unbinned spectra while black lines show the spectra binned to improve the S/N. The instrument used and the phase of each spectrum are shown next to each spectrum.

(The data used to create this figure are available.)

not satisfy our early nebular-phase transition criterion and is excluded from the sample.

SN 2019txr was found close to the nucleus of an irregular spiral galaxy at $z = 0.044$, and peaked at an absolute magnitude of $M_r \approx -16.7$ mag. The peak light spectrum is relatively noisy and we can only identify P-Cygni features of Ca II, O I, and possibly He I; however, we classify it as an SN Ib/c due to the uncertain identification of He I. We cannot identify any Na I D absorption due to the noisy nature of the spectrum. We obtained a nebular-phase spectrum at ≈270 days from peak, which we found to be dominated by host light. We visually identified a weak nebular emission peak around the [O I] transition, but [Ca II] emission was not detected. We show a host-subtracted spectrum of the object matched with `superfit` with the Type Ib SN 2004gq ≈300 days after peak. Although the features are very weak, the host-subtracted spectrum shows the existence of a broad emission feature around [O I] and possible [Ca II]. Given the host-dominated spectrum, we were unable to measure [Ca II]/[O I], but used the detection of [O I] and the weak detection of the nearby [Ca II] line to constrain the [Ca II]/[O I] ratio to <1, excluding it from the Ca-rich sample.

SN 2018fob was found on the spiral arm of a disk galaxy at $z = 0.029$, and peaked at an absolute magnitude of

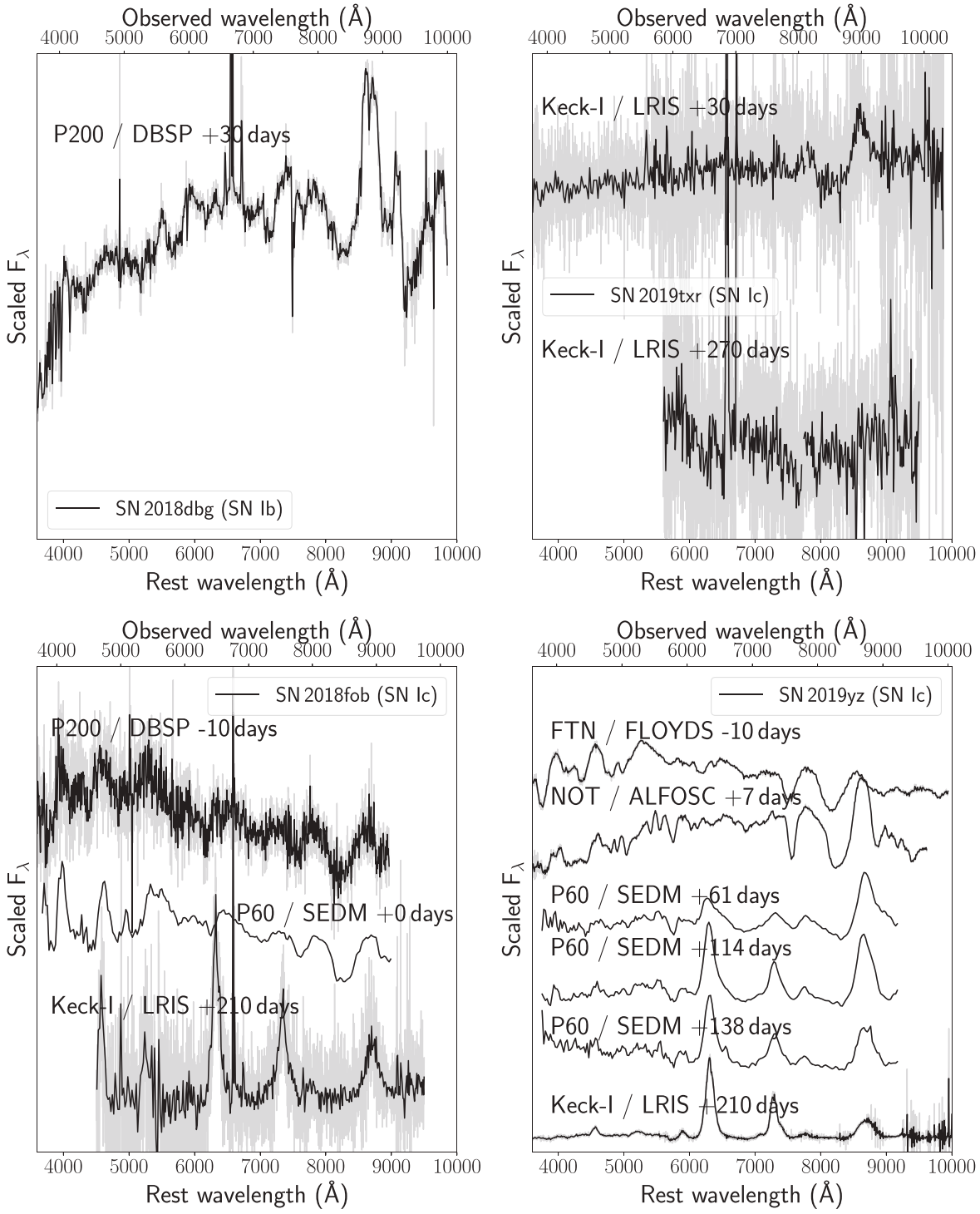

Figure 29. (Continued.)

$M_r \approx -16.9$ mag. The peak light spectra do not show any He signatures, and are consistent with an SN Ic. Na I D absorption is clearly detected at the host redshift, suggesting host extinction. The nebular-phase spectrum at ≈210 days shows a strong [O I] line and a weak [Ca II] line with [Ca II]/[O I] ≈ 0.87, thus excluding it from our sample.

SN 2019yz is the lowest-redshift object in this sample, and is consistent with a reddened SN Ic in the disk of UGC 09977 based on the prominent Na I D absorption in its peak light spectrum. The peak spectrum was obtained from the TNS and was originally obtained by Burke et al. (2019). The light curve peaks at an observed absolute magnitude of $M_r \approx -16.63$ mag. The nebular-phase spectrum at ≈+210 days shows strong [O I] emission with [Ca II]/[O I] ≈ 0.6, excluding it from our sample of Ca-rich events.

SN 2019abb was found on top of an irregular blue galaxy at $z = 0.015$, and peaked at an absolute magnitude of $M_r \approx -16.6$ mag. The peak light spectrum shows characteristic features of an SN Ic with no obvious He signatures, as well as clear Na I D absorption at the host redshift suggesting

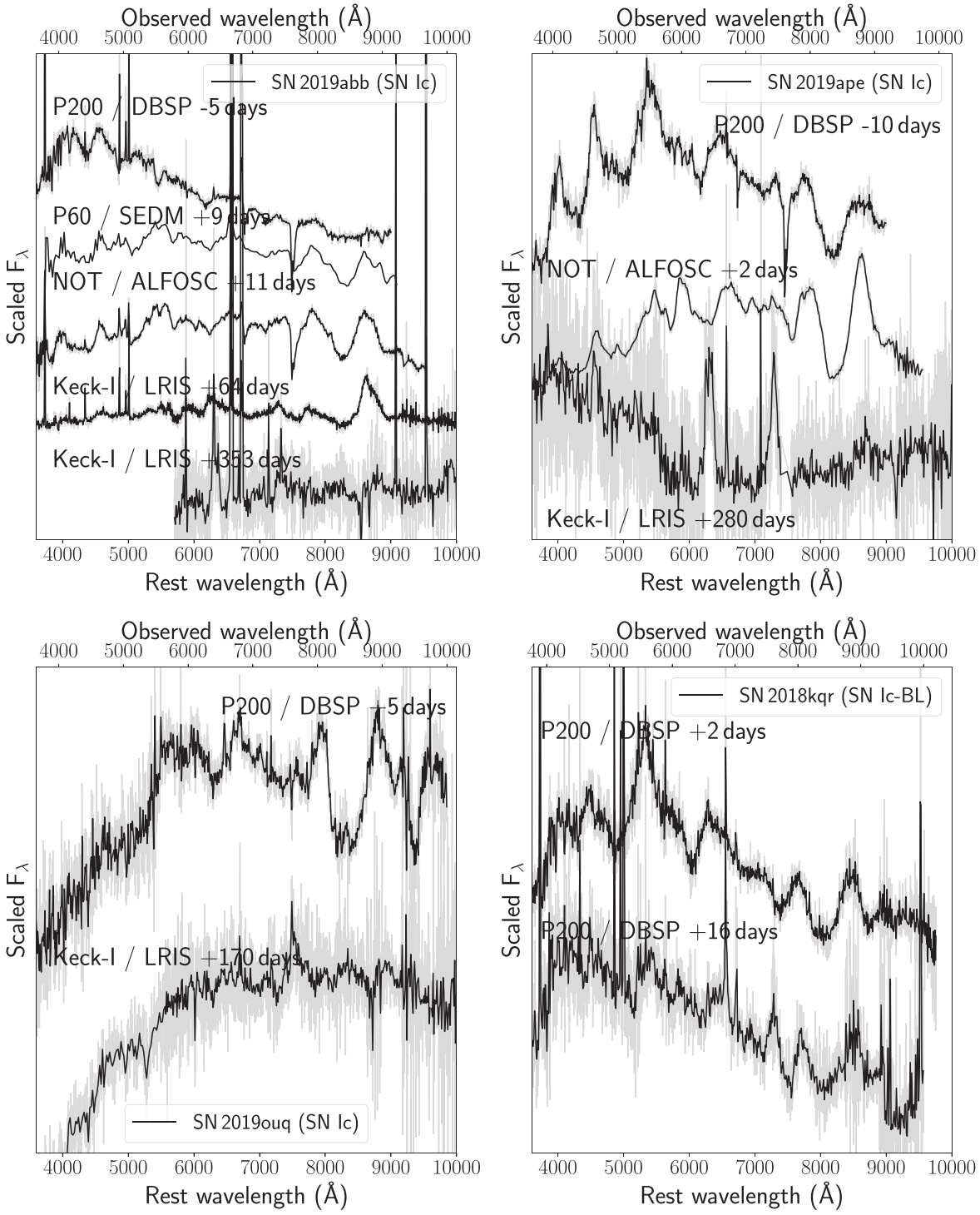

Figure 29. (Continued.)

significant host extinction. A spectrum taken ≈60 days after peak still shows photospheric-phase features suggesting slow spectral evolution. The nebular-phase spectrum obtained at ≈+350 days is dominated by the underlying host, but clearly shows both nebular [O I] and [Ca II] emission lines with [Ca II]/[O I] ≈ 0.8, thus excluding the object from our sample.

SN 2019ape was detected on top of a yellow early-type galaxy at $z = 0.020$, and peaked at an absolute magnitude of $M_r \approx -16.6$ mag. Although the galaxy morphology is early-type, the SDSS and SN spectra show clear Hα emission. The peak light spectrum is characteristic of an SN Ic with no He signatures. Na I D absorption is also detected in the peak light spectrum, confirming host reddening. The nebular-phase spectrum taken at ≈+280 days shows clear [O I] and [Ca II] emission lines with [Ca II]/[O I] ≈ 0.9 thus excluding it from our sample. A complete analysis of this object will be presented in a forthcoming publication (I. Irani et al. 2020, in preparation).

SN 2019ouq was found in the disk of a nearly edge-on disk galaxy at $z = 0.036$, and peaked at an absolute magnitude of

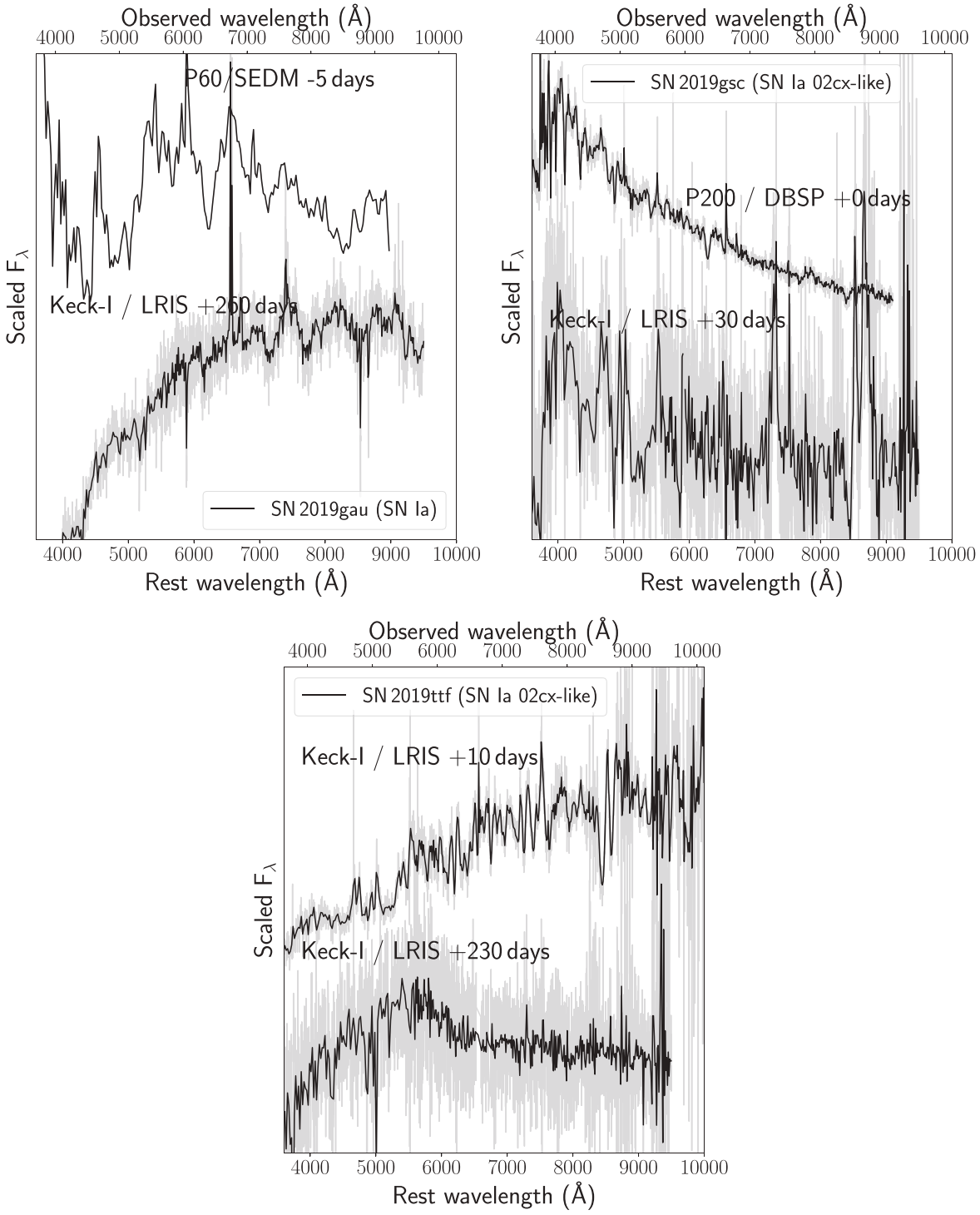

Figure 29. (Continued.)

$M_r \approx -16.9$ mag. The peak light spectrum exhibits a highly reddened continuum but with clear broad P-Cygni features of O I and Ca II. Using `superfit` to subtract the host emission, we found that the peak spectrum is well matched to the Type Ic SN 1994I about 7 days after peak. The same fit suggests that an extinction of $A_V \approx 1$ mag is required to match the continuum. The nebular spectrum obtained at ≈170 days from maximum light is completely dominated by the underlying host galaxy continuum, making it difficult to identify the nebular [O I] and [Ca II] features directly. We thus used `superfit` to subtract the host features and show a host-subtracted spectrum in Figure 30. As shown, the nebular-phase spectrum is consistent with a late-time spectrum of the Type Ic SN 1997ef at ≈281 days. The host-subtracted late-time spectrum also shows similarities to the late-time spectra of the SNe Ic SN 2006aj and SN 1994I. In particular, the host-subtracted spectrum exhibits an [O I] line stronger than the [Ca II] line, constraining [Ca II]/[O I] $\lesssim 1$, thus excluding it from the Ca-rich sample.

SN 2018kqr was detected inside a blue irregular galaxy at $z = 0.045$, and peaked at an absolute magnitude of

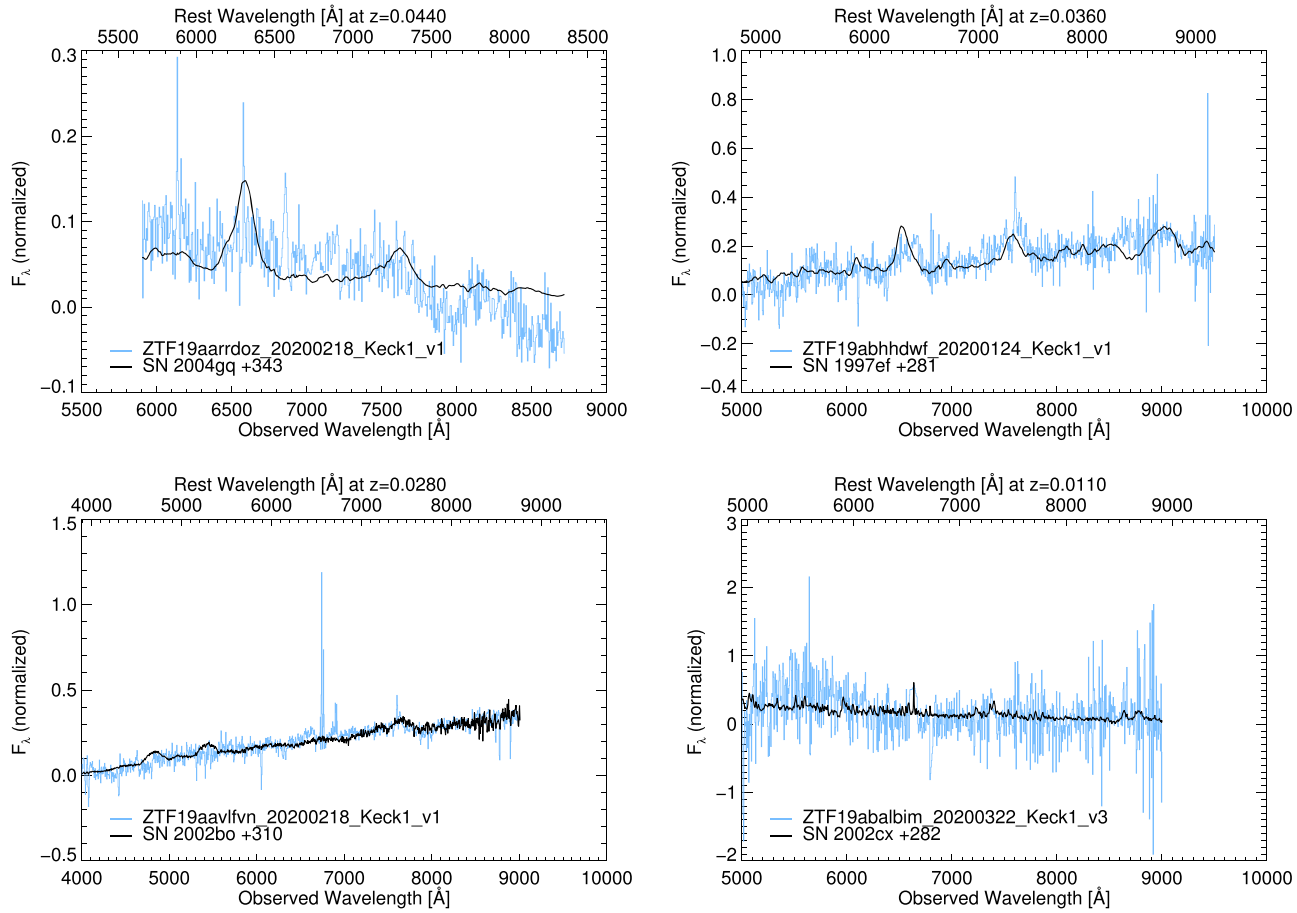

Figure 30. Host-subtracted late-time spectra of events in the sample that are heavily contaminated by host galaxy light and thus require host subtraction using `superfit` (Howell et al. 2005). (Top left) Late-time spectrum of SN 2019txr with host features subtracted using `superfit`. The observed host-subtracted spectrum is shown in blue, while the black line shows the best-match spectrum of the Type Ib SN 2004gq at 297 days after peak. (Top right) Late-time spectrum of SN 2019ouq plotted with the late-time spectrum of Type Ic SN 1997ef at ≈270 days after peak light. (Bottom left) Host-subtracted late-time spectrum of SN 2019gau at ≈270 days, compared against a late-time spectrum of the Type Ia SN 2002bo. However, we do not find a convincing match as several features in the subtracted spectrum are not well matched, and present the fit here for completeness. (Bottom right) Host-subtracted late-time spectrum of SN 2019ttf at ≈210 days compared to the late-time spectrum of SN 2002cx at ≈280 days.

$M_r \approx -16.8$ mag. The peak light spectrum shows broad features consistent with an SN Ic-BL around peak light. Na I D absorption is not clearly detected at the host redshift. We obtained a follow-up spectrum ≈16 days after peak light where the source still exhibits strong photospheric features consistent with an SN Ic. However, we were unable to obtain a follow-up nebular spectrum for this object. Nevertheless, the slow photospheric-phase evolution of this object is consistent with a normal SN Ic, and excludes it from the Ca-rich sample discussed in this work.

SN 2019gau was detected close to the core of a disk galaxy at $z = 0.028$, and peaked at an absolute magnitude of $M_r \approx -16.8$ mag. A low-resolution SEDM spectrum taken near peak shows a strong Si II line and the Ca II NIR triplet in P-Cygni absorption, leading to the SN Ia classification of this event. We obtained a late-time spectrum of the source at ≈260 days from peak, and found it to be dominated by the host galaxy light. We attempted host subtraction using `superfit`, but were unable to find a good match to the host-subtracted features. For completeness, we present the best-fit host-subtracted spectrum in Figure 30 compared to the best match in `superfit` to the late-time spectrum of SN 2002bo. Unlike Ca-Ia objects, which show strong [Ca II] emission and no [O I] emission, this host-subtracted spectrum does not show any strong [Ca II] emission, leading us to exclude it from the Ca-rich sample.

SN 2019gsc was detected inside an irregular blue galaxy at $z = 0.011$, and peaked at a faint absolute magnitude of $M_r = -13.90$ mag. Its peak light spectrum exhibits low-velocity Si II lines similar to those of 02cx-like SNe Ia (Li et al. 2003), while its faint peak luminosity makes it similar to the lowest-luminosity member SN 2008ha (Foley et al. 2009). Our spectrum taken at ≈+30 days from peak is still photospheric and dominated by several low-velocity P-Cygni features. Additional data on SN 2019gsc has been published in Srivastav et al. (2020) and Tomasella et al. (2020), which show that the source does not turn nebular even up to ≈60 days from peak light, consistent with our data and with what is typically observed in this class (Foley et al. 2016). The absence of an early nebular-phase transition excludes it from the Ca-rich sample.

SN 2019ttf was found on top of an irregular star-forming galaxy at $z = 0.011$, and peaked at a faint absolute magnitude of $M_r = -14.0$ mag. The spectrum taken at ≈+10 days from peak shows low-velocity lines similar to those of the 02cx-like SNe Ia SN 2008ha (Foley et al. 2009) and SN 2005hk (Phillips et al. 2007). Its low peak luminosity is similar to that of SN 2019gsc. We obtained a late-time spectrum of the object at

≈230 days, which is dominated by the underlying host galaxy light. We show a host-subtracted spectrum using `superfit` in Figure 30. The subtracted spectrum is relatively noisy, but we note two detected features of Na I and [Ca II] (near 5800 Å and 7300 Å respectively) that are similar to those of SN 2002cx at a similar phase. As in the case of 02cx-like objects that do not become completely nebular at late times, we found a weak Na I P-Cygni profile, and thus exclude this object from the Ca-rich sample.

A.2. Candidate Selection and False Positives

In Section 2.3, we present our selection criteria for identifying candidate Ca-rich gap transients in order to prioritize nebular-phase follow-up. We now evaluate the merits and disadvantages of our selection scheme in the context of understanding the broader population of Ca-rich transients. We start with a comparison of our selection criteria to those of Kasliwal et al. (2012). Unlike that work, we did not select candidates based on their photometric evolution or spectroscopic velocities. This choice made us sensitive to events with broader light curves such as SN 2019pxu, which appears to be a more luminous and slower-evolving member of this class.

However, we did select events based on their peak luminosity, with a cutoff at $M = -17$ mag. We thus caution that certain spectroscopic subtypes may be underrepresented in this sample—e.g., the Ca-Ia events appear to exhibit systematically higher peak luminosity than the Ca-Ib/c events. Indeed, the only Ca-Ia object in the sample SN 2019ofm is also the faintest SN Ia in the CLU sample (barring the low-velocity 08ha-like events), suggesting that the Ca-Ia events discussed here could represent the tip of the Ca-rich sample in the broader 91bg-like SN Ia population. Resolving this issue would require a similar experiment targeting brighter SNe Ia, which will inevitably include other known populations of faint SNe Ia.

As in Kasliwal et al. (2012), we did not select events based on their spectroscopic type at peak light. However, the low spectroscopic velocities in SN 2018kjy would not have passed the criteria in Kasliwal et al. (2012) since they required "normal" photospheric-phase velocities. Our follow-up campaign revealed that despite its peculiar low spectroscopic velocities at peak, the later evolution of SN 2018kjy establishes its membership in the class of Ca-rich gap transients. In the context of low-velocity events, it is important to highlight the contamination of 02cx-like SNe Ia. Two of the events in the control sample are spectroscopically similar to 02cx-like objects near peak light (similar to SN 2008ha; Foley et al. 2009) with low spectroscopic velocities at peak (like SN 2018kjy). Yet unlike that of SN 2018kjy (and the rest of the Ca-rich class), their spectra do not turn nebular at late phases and exhibit a pseudo-continuum of emission lines.

Next, we discuss the host environments of these events, reiterating that our selection criteria are agnostic to the host type and environment. In comparison to the SNe Ib/c in the control sample (which were primarily found in star-forming late-type galaxies), a striking characteristic of the sample of Ca-Ib/c objects is their preference for early-type galaxies and old environments. SN 2019pxu is the only exception, but is still at a large projected offset of ≈18 kpc from its host, suggesting that spectroscopically classified SNe Ib/c in old environments could be used to select likely Ca-rich gap transients near peak light. Yet, SN 2019ape serves as an important exception to this trend as an SN Ic in an early-type galaxy, suggesting that this criterion also has its own false positives despite producing a relatively high success rate (six out of seven SNe Ib/c in early-type galaxies in this sample turned out to be Ca-rich events). However, nearly all the low-luminosity SNe Ia in the sample (including two 02cx-like events) are in late-type galaxies—as such, the environment of the only Ca-Ia event in the sample SN 2019ofm is not exceptional.

In terms of the photometric and spectroscopic properties of the transients, the sample presented in this work was selected using the smallest possible selection criteria to identify these faint transients in the local universe. The final confirmation of a Ca-rich gap transient, however, was derived from nebular-phase spectroscopy at late times. As such, it is instructive to examine if the confirmed sample of Ca-rich gap transients can be differentiated based on the peak light spectra and photometric evolution in order to guide future searches for these events. In Figure 15, we show the luminosity–width phase space of the control sample of transients compared to the Ca-rich gap transients analyzed in this work. We make this comparison in order to examine if Ca-rich gap transients can be identified from their peak luminosity and light-curve evolution near peak. As shown, a striking trend is that the control sample of objects exhibit systematically slower-evolving light curves (smaller Δm_7 and longer $t_{\rm f,1/2}$) than nearly the entire sample of Ca-rich gap transients, suggesting typically longer diffusion time and correspondingly larger ejecta masses in the control sample. Yet, the Ca-rich and control objects occupy a common phase space near $\Delta m_7 \approx 0.3$ and $M_{\rm p}$ between -16 and -17, meaning that the fastest-evolving objects in this sample are always Ca-rich. Thus, we conclude that while the fastest-evolving Ca-rich gap transients $\Delta m_7 > 0.4$ can be identified with peak light photometry and spectroscopy, it is difficult to select a complete sample based on only these properties.

The broader light curves and low [Ca II]/[O I] of the Type Ib/c events in the control sample suggest that these events are likely consistent with being normal core-collapse SNe (Gal-Yam 2017) that are extinguished by foreground dust. Indeed, the detection of prominent Na I D absorption from the host galaxy in nearly all of these events suggests that host extinction likely plays an important role in making these events appear subluminous at peak similar to Ca-rich events. The 02cx-like events (Li et al. 2003) are consistent with very low luminosity members of the SN Iax class similar to the lowest-luminosity member SN 2008ha (Foley et al. 2009). However, we did not have a high-resolution spectrum of the only other Type Ia SN 2019gau at peak to ascertain the role of host extinction. At the same time, we were unable to securely identify nebular emission features in the late-time spectrum of this object, leaving this as an inconclusive low-luminosity SN Ia in the sample.

We examined the spectroscopic properties of the control sample to identify potential spectroscopic clues at peak light for identifying Ca-rich gap transients. Ca-Ib exhibit spectra strikingly similar to those of normal SNe Ib in the sample; however, line-blanketed spectra of the red Ca-Ib objects are uncommon in the control sample. The only objects in the control sample that also exhibit suppressed blue continua are SN 2019txl and SN 2019mjo. The former object also exhibits strong Na I D absorption, suggesting that host extinction likely

suppresses the blue continuum in this otherwise normal core-collapse SN. SN 2019mjo is a peculiar SN Ib whose nature remains unclear, and we do not discuss its properties further here. Nevertheless, peculiar low-velocity objects such as SN 2018kjr and PTF 12bho are not seen in the control sample, suggesting that the combination of low velocity and a highly reddened continuum may be indicative of a Ca-rich object if its peak luminosity can be constrained. Ca-Ia objects with strongly line-blanketed spectra are unique in the broader population of SNe Ia that exhibit blue continua at peak (see the discussion in De et al. 2019b), and thus strong line blanketing with prominent Si II lines could be used to identify likely Ca-Ia candidates at peak. Given that all the above selection procedures were unable to yield a complete sample of Ca-rich gap transients, we conclude that in general nebular-phase spectroscopy of systematically selected samples of low-luminosity transients in the local universe with 8–10 m class telescopes will continue to be important for our census of these elusive transients.

ORCID iDs

Kishalay De https://orcid.org/0000-0002-8989-0542
Mansi M. Kasliwal https://orcid.org/0000-0002-5619-4938
Anastasios Tzanidakis https://orcid.org/0000-0003-0484-3331
U. Christoffer Fremling https://orcid.org/0000-0002-4223-103X
Robert Aloisi https://orcid.org/0000-0003-2822-616X
Igor Andreoni https://orcid.org/0000-0002-8977-1498
Eric C. Bellm https://orcid.org/0000-0001-8018-5348
David O. Cook https://orcid.org/0000-0002-6877-7655
Dmitry Duev https://orcid.org/0000-0001-5060-8733
Alison Dugas https://orcid.org/0000-0001-7344-0208
Sara Frederick https://orcid.org/0000-0001-9676-730X
Avishay Gal-Yam https://orcid.org/0000-0002-3653-5598
Daniel Goldstein https://orcid.org/0000-0003-3461-8661
V. Zach Golkhou https://orcid.org/0000-0001-8205-2506
Matthew J. Graham https://orcid.org/0000-0002-3168-0139
Matthew Hankins https://orcid.org/0000-0001-9315-8437
George Helou https://orcid.org/0000-0003-3367-3415
Anna Y. Q. Ho https://orcid.org/0000-0002-9017-3567
Ido Irani https://orcid.org/0000-0002-7996-8780
Jacob E. Jencson https://orcid.org/0000-0001-5754-4007
David L. Kaplan https://orcid.org/0000-0001-6295-2881
S. R. Kulkarni https://orcid.org/0000-0001-5390-8563
Thomas Kupfer https://orcid.org/0000-0002-6540-1484
Russ R. Laher https://orcid.org/0000-0003-2451-5482
Ragnhild Lunnan https://orcid.org/0000-0001-9454-4639
Frank J. Masci https://orcid.org/0000-0002-8532-9395
Adam A. Miller https://orcid.org/0000-0001-9515-478X
James D. Neill https://orcid.org/0000-0002-0466-1119
Eran O. Ofek https://orcid.org/0000-0002-6786-8774
Daniel A. Perley https://orcid.org/0000-0001-8472-1996
Abigail Polin https://orcid.org/0000-0002-1633-6495
Thomas A. Prince https://orcid.org/0000-0002-8850-3627
Eliot Quataert https://orcid.org/0000-0001-9185-5044
Reed L. Riddle https://orcid.org/0000-0002-0387-370X
Ben Rusholme https://orcid.org/0000-0001-7648-4142
Yashvi Sharma https://orcid.org/0000-0003-4531-1745
David L. Shupe https://orcid.org/0000-0003-4401-0430
Jesper Sollerman https://orcid.org/0000-0003-1546-6615
Leonardo Tartaglia https://orcid.org/0000-0003-3433-1492
Lin Yan https://orcid.org/0000-0003-1710-9339
Yuhan Yao https://orcid.org/0000-0001-6747-8509

References

Abolfathi, B., Aguado, D. S., Aguilar, G., et al. 2018, ApJS, 235, 42
Abraham, R. G., & van Dokkum, P. G. 2014, PASP, 126, 55
Arnett, W. D. 1982, ApJ, 253, 785
Arnett, W. D., Branch, D., & Wheeler, J. C. 1985, Natur, 314, 337
Astropy Collaboration, Robitaille, T. P., Tollerud, E. J., et al. 2013, A&A, 558, A33
Barbary, K., Barclay, T., Biswas, R., et al. 2016, SNCosmo: Python Library for Supernova Cosmology, Astrophysics Source Code Library, ascl:1611.017
Bauer, E. B., Schwab, J., & Bildsten, L. 2017, ApJ, 845, 97
Bell, E. F., McIntosh, D. H., Katz, N., & Weinberg, M. D. 2003, ApJS, 149, 289
Bellm, E. C., Kulkarni, S. R., Barlow, T., et al. 2019b, PASP, 131, 068003
Bellm, E. C., Kulkarni, S. R., Graham, M. J., et al. 2019a, PASP, 131, 018002
Bellm, E. C., & Sesar, B. 2016, pyraf-dbsp: Reduction pipeline for the Palomar Double Beam Spectrograph, Astrophysics Source Code Library, ascl:1602.002
Bertin, E. 2006, in ASP Conf. Ser. 351, Astronomical Data Analysis Software and Systems XV, ed. C. Gabriel et al. (San Francisco, CA: ASP), 112
Bertin, E. 2011, in ASP Conf. Ser. 442, Astronomical Data Analysis Software and Systems XX, ed. I. N. Evans et al. (San Francisco, CA: ASP), 435
Bertin, E., & Arnouts, S. 1996, A&AS, 117, 393
Bertin, E., Mellier, Y., Radovich, M., et al. 2002, in ASP Conf. Ser. 281, Astronomical Data Analysis Software and Systems XI, ed. D. A. Bohlender, D. Durand, & T. H. Handley (San Francisco, CA: ASP), 228
Bildsten, L., Shen, K. J., Weinberg, N. N., & Nelemans, G. 2007, ApJL, 662, L95
Blagorodnova, N., Neill, J. D., Walters, R., et al. 2018, PASP, 130, 035003
Blondin, S., & Tonry, J. L. 2007, ApJ, 666, 1024
Bloom, J. S., Kulkarni, S. R., & Djorgovski, S. G. 2002, AJ, 123, 1111
Bobrick, A., Davies, M. B., & Church, R. P. 2017, MNRAS, 467, 3556
Brooks, J., Bildsten, L., Marchant, P., & Paxton, B. 2015, ApJ, 807, 74
Brown, W. R., Kilic, M., Kenyon, S. J., & Gianninas, A. 2016, ApJ, 824, 46
Burke, J., Arcavi, I., Hiramatsu, D., et al. 2019, TNSCR, 2019-1232, 1
Cano, Z. 2013, MNRAS, 434, 1098
Cao, Y., Kasliwal, M. M., Arcavi, I., et al. 2013, ApJL, 775, L7
Cardelli, J. A., Clayton, G. C., & Mathis, J. S. 1989, ApJ, 345, 245
Carter, P. J., Marsh, T. R., Steeghs, D., et al. 2013, MNRAS, 429, 2143
Chambers, K. C., Huber, M. E., Flewelling, H., et al. 2018, TNSTR, 2018-2068, 1
Chambers, K. C., Magnier, E. A., Metcalfe, N., et al. 2016, arXiv:1612.05560
Chen, P., Dong, S., Stritzinger, M. D., et al. 2020, ApJL, 889, L6
Clayton, G. C. 1996, PASP, 108, 225
Cook, D. O., Kasliwal, M. M., Van Sistine, A., et al. 2019, ApJ, 880, 7
Crts, N. M. W. 2018, TNSTR, 2018-804, 1
Dálya, G., Galgóczi, G., Dobos, L., et al. 2018, MNRAS, 479, 2374
De, K. 2019a, TNSTR, 2019-2208, 1
De, K. 2019b, TNSTR, 2019-2307, 1
De, K., Hankins, M. J., Kasliwal, M. M., et al. 2020, PASP, 132, 025001
De, K., Kasliwal, M. M., Cantwell, T., et al. 2018a, ApJ, 866, 72
De, K., Kasliwal, M. M., Ofek, E. O., et al. 2018b, Sci, 362, 201
De, K., Kasliwal, M. M., Polin, A., et al. 2019b, ApJL, 873, L18
De, K., Tzanidakis, A., Kasliwal, M. M., Fremling, C., & Kulkarni, S. R. 2019a, ATel, 13262, 1
Dekany, R., Smith, R. M., Belicki, J., et al. 2016, Proc. SPIE, 9908, 99085M
DESI Collaboration, Aghamousa, A., Aguilar, J., et al. 2016, arXiv:1611.00036
Dessart, L., & Hillier, D. J. 2015, MNRAS, 447, 1370
Dessart, L., Hillier, D. J., Li, C., & Woosley, S. 2012, MNRAS, 424, 2139
Dey, A., Schlegel, D. J., Lang, D., et al. 2019, AJ, 157, 168
Dimitriadis, G., Siebert, M. R., Kilpatrick, C. D., et al. 2019, TNSCR, 2019-675, 1
Drake, A. J., Djorgovski, S. G., Mahabal, A., et al. 2009, ApJ, 696, 870
Drout, M. R., Soderberg, A. M., Gal-Yam, A., et al. 2011, ApJ, 741, 97
D'Souza, R., Kauffman, G., Wang, J., & Vegetti, S. 2014, MNRAS, 443, 1433
Duev, D. A., Mahabal, A., Masci, F. J., et al. 2019, MNRAS, 489, 3582
Feindt, U., Nordin, J., Rigault, M., et al. 2019, JCAP, 2019, 005
Filippenko, A. V. 1997, ARA&A, 35, 309
Filippenko, A. V., Chornock, R., Swift, B., et al. 2003, IAUC, 8159
Filippenko, A. V., Richmond, M. W., Branch, D., et al. 1992, AJ, 104, 1543
Fink, M., Röpke, F. K., Hillebrandt, W., et al. 2010, A&A, 514, A53

Flörs, A., Spyromilio, J., Taubenberger, S., et al. 2020, MNRAS, 491, 2902
Foley, R. J. 2015, MNRAS, 452, 2463
Foley, R. J., Chornock, R., Filippenko, A. V., et al. 2009, AJ, 138, 376
Foley, R. J., Jha, S. W., Pan, Y.-C., et al. 2016, MNRAS, 461, 433
Fransson, C., & Chevalier, R. A. 1989, ApJ, 343, 323
Fremling, C., Sollerman, J., Kasliwal, M. M., et al. 2018, A&A, 618, A37
Fremling, C., Sollerman, J., Taddia, F., et al. 2016, A&A, 593, A68
Fremling, U. C., Miller, A. A., Sharma, Y., et al. 2019, arXiv:1910.12973
Frohmaier, C., Sullivan, M., Maguire, K., & Nugent, P. 2018, ApJ, 858, 50
Frohmaier, C., Sullivan, M., Nugent, P. E., et al. 2019, MNRAS, 486, 2308
Frohmaier, C., Sullivan, M., Nugent, P. E., Goldstein, D. A., & DeRose, J. 2017, ApJS, 230, 4
Fryer, C. L., Ruiter, A. J., Belczynski, K., et al. 2010, ApJ, 725, 296
Gaia Collaboration, Brown, A. G. A., Vallenari, A., et al. 2018, A&A, 616, A1
Galbany, L., Ashall, C., Höflich, P., et al. 2019, A&A, 630, A76
Gal-Yam, A. 2017, in Handbook of Supernovae, ed. A. Alsabti & P. Murdin (Cham: Springer), 1
Gal-Yam, A., Arcavi, I., Ofek, E. O., et al. 2014, Natur, 509, 471
Geier, S., Marsh, T. R., Wang, B., et al. 2013, A&A, 554, A54
Graham, M. J., Kulkarni, S. R., Bellm, E. C., et al. 2019, PASP, 131, 078001
Grzegorzek, J. 2019, TNSTR, 2019-666, 1
Guillochon, J., Parrent, J., Kelley, L. Z., & Margutti, R. 2017, ApJ, 835, 64
Hachinger, S., Mazzali, P. A., Taubenberger, S., et al. 2012, MNRAS, 422, 70
Harris, W. E. 1996, AJ, 112, 1487
Hinshaw, G., Larson, D., Komatsu, E., et al. 2013, ApJS, 208, 19
Hoeflich, P., & Khokhlov, A. 1996, ApJ, 457, 500
Hogg, D. W., Pahre, M. A., McCarthy, J. K., et al. 1997, MNRAS, 288, 404
Holcomb, C., Guillochon, J., De Colle, F., & Ramirez-Ruiz, E. 2013, ApJ, 771, 14
Howell, D. A. 2001, ApJL, 554, L193
Howell, D. A., Sullivan, M., Perrett, K., et al. 2005, ApJ, 634, 1190
Hunter, J. D. 2007, CSE, 9, 90
Iben, I, Jr., & Tutukov, A. V. 1989, ApJ, 342, 430
Inserra, C., Sim, S. A., Wyrzykowski, L., et al. 2015, ApJL, 799, L2
Jacobson-Galán, W. V., Polin, A., Foley, R. J., et al. 2020, ApJ, 896, 165
Jerkstrand, A. 2017, in Handbook of Supernovae, ed. A. W. Alsabti & P. Murdin (Cham: Springer), 795
Jiang, J.-A., Doi, M., Maeda, K., et al. 2017, Natur, 550, 80
Kasliwal, M. M., Cannella, C., Bagdasaryan, A., et al. 2019, PASP, 131, 038003
Kasliwal, M. M., Kulkarni, S. R., Gal-Yam, A., et al. 2010, ApJL, 723, L98
Kasliwal, M. M., Kulkarni, S. R., & Gal-Yam, A. 2012, ApJ, 755, 161
Kawabata, K. S., Maeda, K., Nomoto, K., et al. 2010, Natur, 465, 326
Kawana, K., Maeda, K., Yoshida, N., & Tanikawa, A. 2020, ApJL, 890, L26
Khatami, D. K., & Kasen, D. N. 2019, ApJ, 878, 56
Kochanek, C. S., Pahre, M. A., Falco, E. E., et al. 2001, ApJ, 560, 566
Kollmeier, J. A., Zasowski, G., Rix, H.-W., et al. 2017, arXiv:1711.03234
Kromer, M., Sim, S. A., Fink, M., et al. 2010, ApJ, 719, 1067
Kulkarni, S. R., Perley, D. A., & Miller, A. A. 2018, ApJ, 860, 22
Kupfer, T., van Roestel, J., Brooks, J., et al. 2017, ApJ, 835, 131
Lang, D., Hogg, D. W., & Schlegel, D. J. 2016, AJ, 151, 36
Leadbeater, R. 2018, TNSCR, 2018-1486, 1
Li, W., Filippenko, A. V., Chornock, R., et al. 2003, PASP, 115, 453
Li, W., Leaman, J., Chornock, R., et al. 2011, MNRAS, 412, 1441
Liu, Y.-Q., Modjaz, M., Bianco, F. B., & Graur, O. 2016, ApJ, 827, 90
Livne, E., & Arnett, D. 1995, ApJ, 452, 62
Livne, E., & Glasner, A. S. 1990, ApJ, 361, 244
Livne, E., & Glasner, A. S. 1991, ApJ, 370, 272
Lucy, L. B. 1991, ApJ, 383, 308
Lunnan, R., Kasliwal, M. M., Cao, Y., et al. 2017, ApJ, 836, 60
Lyman, J. D., Levan, A. J., Church, R. P., Davies, M. B., & Tanvir, N. R. 2014, MNRAS, 444, 2157
Lyman, J. D., Levan, A. J., James, P. A., et al. 2016, MNRAS, 458, 1768
MacLeod, M., Goldstein, J., Ramirez-Ruiz, E., Guillochon, J., & Samsing, J. 2014, ApJ, 794, 9
MacLeod, M., Guillochon, J., Ramirez-Ruiz, E., Kasen, D., & Rosswog, S. 2016, ApJ, 819, 3
Mahabal, A., Rebbapragada, U., Walters, R., et al. 2019, PASP, 131, 038002
Mannucci, F., Maoz, D., Sharon, K., et al. 2008, MNRAS, 383, 1121
Margalit, B., & Metzger, B. D. 2016, MNRAS, 461, 1154
Marinacci, F., Vogelsberger, M., Pakmor, R., et al. 2018, MNRAS, 480, 5113
Marion, G. H., Vinko, J., Kirshner, R. P., et al. 2014, ApJ, 781, 69
Masci, F. J., Laher, R. R., Rusholme, B., et al. 2019, PASP, 131, 018003
McBrien, O. R., Smartt, S. J., Chen, T.-W., et al. 2019, ApJL, 885, L23
McKinney, W. 2010, in Proc. 9th Python in Science Conf., ed. S. van der Walt & J. Millman, 51, http://conference.scipy.org/proceedings/scipy2010/mckinney.html
Meng, X., & Han, Z. 2015, A&A, 573, A57
Mernier, F., de Plaa, J., Pinto, C., et al. 2016, A&A, 595, A126
Metzger, B. D. 2012, MNRAS, 419, 827
Milisavljevic, D., Patnaude, D. J., Raymond, J. C., et al. 2017, ApJ, 846, 50
Moore, K., Townsley, D. M., & Bildsten, L. 2013, ApJ, 776, 97
Moriya, T. J., Mazzali, P. A., Tominaga, N., et al. 2017, MNRAS, 466, 2085
Mulchaey, J. S., Kasliwal, M. M., & Kollmeier, J. A. 2014, ApJL, 780, L34
Naiman, J. P., Pillepich, A., Springel, V., et al. 2018, MNRAS, 477, 1206
Neill, J. D., Sullivan, M., Howell, D. A., et al. 2009, ApJ, 707, 1449
Nelemans, G., Yungelson, L. R., & Portegies Zwart, S. F. 2004, MNRAS, 349, 181
Nelson, D., Springel, V., Pillepich, A., et al. 2019, ComAC, 6, 2
Nomoto, K. 1980, SSRv, 27, 563
Nomoto, K. 1982a, ApJ, 253, 798
Nomoto, K. 1982b, ApJ, 257, 780
Nordin, J., Brinnel, V., Giomi, M., et al. 2019a, TNSTR, 2019-1594, 1
Nordin, J., Brinnel, V., van Santen, J., et al. 2019b, A&A, 631, A147
Nugent, P., Baron, E., Branch, D., Fisher, A., & Hauschildt, P. H. 1997, ApJ, 485, 812
Nugent, P. E., Sullivan, M., Cenko, S. B., et al. 2011, Natur, 480, 344
Oke, J. B., Cohen, J. G., Carr, M., et al. 1995, PASP, 107, 375
Oke, J. B., & Gunn, J. E. 1982, PASP, 94, 586
Pakmor, R., Kromer, M., Taubenberger, S., & Springel, V. 2013, ApJL, 770, L8
Patterson, M. T., Bellm, E. C., Rusholme, B., et al. 2019, PASP, 131, 018001
Perets, H. B. 2014, arXiv:1407.2254
Perets, H. B., Gal-yam, A., Crockett, R. M., et al. 2011, ApJL, 728, L36
Perets, H. B., Gal-Yam, A., Mazzali, P. A., et al. 2010, Natur, 465, 322
Perley, D. A. 2019, PASP, 131, 084503
Pfahl, E., Scannapieco, E., & Bildsten, L. 2009, ApJL, 695, L111
Phillips, M. M. 1993, ApJL, 413, L105
Phillips, M. M., Li, W., Frieman, J. A., et al. 2007, PASP, 119, 360
Piro, A. L., & Nakar, E. 2014, ApJ, 784, 85
Polin, A., Nugent, P., & Kasen, D. 2019a, ApJ, 873, 84
Polin, A., Nugent, P., & Kasen, D. 2019b, arXiv:1910.12434
Prentice, S. J., Maguire, K., Flörs, A., et al. 2020, A&A, 635, A186
Rigault, M., Neill, J. D., Blagorodnova, N., et al. 2019, A&A, 627, A115
Roelofs, G. H. A., Nelemans, G., & Groot, P. J. 2007, MNRAS, 382, 685
Rosswog, S., Ramirez-Ruiz, E., & Hix, W. R. 2008, ApJ, 679, 1385
Samsing, J., MacLeod, M., & Ramirez-Ruiz, E. 2017, ApJ, 846, 36
Schlafly, E. F., & Finkbeiner, D. P. 2011, ApJ, 737, 103
Schwab, J. 2019, ApJ, 885, 27
Sell, P. H., Arur, K., Maccarone, T. J., et al. 2018, MNRAS, 475, L111
Sell, P. H., Maccarone, T. J., Kotak, R., Knigge, C., & Sand, D. J. 2015, MNRAS, 450, 4198
Shen, K. J., & Bildsten, L. 2009, ApJ, 699, 1365
Shen, K. J., Kasen, D., Weinberg, N. N., Bildsten, L., & Scannapieco, E. 2010, ApJ, 715, 767
Shen, K. J., & Moore, K. 2014, ApJ, 797, 46
Shen, K. J., Quataert, E., & Pakmor, R. 2019, ApJ, 887, 180
Silverman, J. M., Foley, R. J., Filippenko, A. V., et al. 2012, MNRAS, 425, 1789
Silverman, J. M., Mazzali, P., Chornock, R., et al. 2009, PASP, 121, 689
Sim, S. A., Fink, M., Kromer, M., et al. 2012, MNRAS, 420, 3003
Sim, S. A., Röpke, F. K., Hillebrandt, W., et al. 2010, ApJL, 714, L52
Srivastav, S., Smartt, S. J., Leloudas, G., et al. 2020, ApJL, 892, L24
Sullivan, M., Kasliwal, M. M., Nugent, P. E., et al. 2011, ApJ, 732, 118
Sullivan, M., Le Borgne, D., Pritchet, C. J., et al. 2006, ApJ, 648, 868
Sun, F., & Gal-Yam, A. 2017, arXiv:1707.02543
Tachibana, Y., & Miller, A. A. 2018, PASP, 130, 128001
Taddia, F., Stritzinger, M. D., Bersten, M., et al. 2018, A&A, 609, A136
Taubenberger, S. 2017, in Handbook of Supernovae, ed. A. W. Alsabti & P. Murdin (Cham: Springer), 317
Tauris, T. M., Langer, N., & Podsiadlowski, P. 2015, MNRAS, 451, 2123
Tomasella, L., Stritzinger, M., Benetti, S., et al. 2020, MNRAS, 496, 1132
Tonry, J., Denneau, L., Heinze, A., et al. 2019a, TNSTR, 2019-1035, 1
Tonry, J., Denneau, L., Heinze, A., et al. 2019b, TNSTR, 2019-1787, 1
Tonry, J. L., Denneau, L., Heinze, A. N., et al. 2018, PASP, 130, 064505
Toonen, S., Perets, H. B., Igoshev, A. P., Michaely, E., & Zenati, Y. 2018, A&A, 619, A53
Townsley, D. M., Moore, K., & Bildsten, L. 2012, ApJ, 755, 4
Valenti, S., Yuan, F., Taubenberger, S., et al. 2014, MNRAS, 437, 1519

van Dokkum, P., Abraham, R., Brodie, J., et al. 2016, ApJL, 828, L6
van Dokkum, P., Abraham, R., Romanowsky, A. J., et al. 2017, ApJL, 844, L11
van Dokkum, P., Cohen, Y., Danieli, S., et al. 2018, ApJL, 856, L30
Virtanen, P., Gommers, R., Oliphant, T. E., et al. 2020, NatMe, 17, 261
Waldman, R., Sauer, D., Livne, E., et al. 2011, ApJ, 738, 21
Wiggins, P. 2018, TNSTR, 2018-1459, 1
Woosley, S. E. 2019, ApJ, 878, 49
Woosley, S. E., & Kasen, D. 2011, ApJ, 734, 38
Woosley, S. E., Taam, R. E., & Weaver, T. A. 1986, ApJ, 301, 601
Woosley, S. E., & Weaver, T. A. 1994, ApJ, 423, 371
Yao, Y., Miller, A. A., Kulkarni, S. R., et al. 2019, ApJ, 886, 152
Yaron, O., & Gal-Yam, A. 2012, PASP, 124, 668
Yuan, F., Kobayashi, C., Schmidt, B. P., et al. 2013, MNRAS, 432, 1680
Zackay, B., Ofek, E. O., & Gal-Yam, A. 2016, ApJ, 830, 27
Zenati, Y., Perets, H. B., & Toonen, S. 2019, MNRAS, 486, 1805